Numerical and experimental investigations of surface roughness in 1D photonic crystals

2008 J. Phys.: Condens. Matter 20 454220

(http://iopscience.iop.org/0953-8984/20/45/454220)

IOP PUBLISHING JOURNAL OF PHYSICS: CONDENSED MATTER

J. Phys.: Condens. Matter **20** (2008) 454220 (7pp) doi:10.1088/0953-8984/20/45/454220

Numerical and experimental investigations of surface roughness in 1D photonic crystals

O Glushko[1], R Meisels[1], F Kuchar[1] and R Danzer[2]

[1] Institut für Physik, Montanuniversität Leoben, A-8700 Leoben, Austria
[2] Institut für Struktur- und Funktionskeramik, Montanuniversität Leoben, A-8700 Leoben, Austria

E-mail: oleksandr.glushko@unileoben.ac.at

Received 5 June 2008, in final form 10 September 2008
Published 23 October 2008
Online at stacks.iop.org/JPhysCM/20/454220

Abstract

We present numerical simulations as well as experimental investigations of 1D photonic crystals (PhC) with intentionally introduced surface roughness. An 'experimental simulation' of the roughness was created by gluing alumina powder to both sides of each alumina plate in an alumina–air structure. Transmission experiments were performed on this 1D PhC at microwave frequencies. A 'red-shift' of the band edges observed in experiment and simulation is explained by an increase of the effective thickness of the alumina layers as the surface roughness becomes stronger. The influence of the features of the roughness becomes visible in the simulations only at wavelengths short enough to be of the order of the dimensions of these features. Then, the band edges are smeared and the residual transmission in the band gaps is increased. We show that the main effect responsible for the smearing of the band edges is the scattering of the wave on roughness features. Even for very strong roughness (40% of the plate thickness) the band gaps are not destroyed completely.

(Some figures in this article are in colour only in the electronic version)

1. Introduction

Photonic crystals (PhC) have been intensively investigated since the end of the 1980s when the possibility of the existence of photonic band gaps in periodic dielectric lattices was predicted [1] and then demonstrated first by numerical simulation [2] and experimentally [3]. During the last years the development of this area is characterized by the tendency to miniaturization of photonic crystals with the main aim to scale down the working range to the near IR and visible regions. It is evident that more and more precise fabrication techniques are required for the realization of this task. Thus, the problem of the influence of disorder on the properties of photonic crystals has attracted a great deal of attention. Since defects and inaccuracies in the determination of the geometrical parameters of real structures are inevitable phenomena in sub-micrometer fabrication, the disorder-induced modifications of photonic crystal properties must be taken into account. Since the existence of photonic band gaps in a photonic crystal is a consequence of the periodicity of the refractive index, disturbing that periodicity should result in a modification of the photonic band structure and finally in the disappearance of the band gaps.

Disorder in PhCs can be essentially classified into three types: positional disorder, size/shape disorder, and refractive index disorder. Examples of these deviations from the perfect case for a one-dimensional (1D) photonic crystal, studied so far, are described below.

The reflectance spectra of silicon/air 1D PhC with disorder in thickness were measured in [4]. Disorder was introduced by changing the thickness of three of a total of 11 silicon layers. According to transfer-matrix method (TMM) calculations, the authors claim that three discrete band gaps (4.5–5.5, 6.3–9.2 and 12.8–20.5 μm) related to the periodic (perfect) structure are joined together and form a new wider band gap ranging from 4.5 to 20.5 μm. However, the experimental reflection in this range was significantly lower than unity. The authors attributed it to a deviation of the fabricated structure from the

designed one. In the theoretical work [5] the authors also reported on a band gap extension with increasing disorder. The dielectric constants of the consecutive layers were $\varepsilon_1 = 10.24$ and $\varepsilon_2 = 1.32$ and the structure had 24 periods. Their TMM calculations showed that the transmission band between the band gaps could be totally turned into a high reflection regime ($R > 95\%$). However, in the papers [6, 7] and [8] the authors come to the conclusion that the general effect of the disorder in thickness and refractive index is a smearing of the band edges and a reduction of the width of the band gaps with increasing disorder in 1D PhC.

The influence of interfacial roughness on the reflectance in the center of a photonic band gap of a stack of quarter-wave plates for normal incidence was investigated theoretically in [9]. The main effect reported was a decrease of the reflectivity with increasing rms surface roughness. In [10] a homogenization approximation was applied, where the interfacial region is discretized into thin strips oriented parallel to the surface. The dielectric constant is averaged within each strip. Thus, the dielectric constant of the interfacial region gradually decreases in the direction normal to the surface and is homogeneous in the direction parallel to the surface. The TMM method was used to calculate the reflection of the same structures as used in [9]. Good agreement between the TMM with the homogenization approximation and FDTD calculations of reflection was observed for refractive index contrast $n_1/n_2 < 1.75$. The conclusion was that the reduction of the reflectance due to surface roughness is a consequence of collective smearing of the interfaces rather than of the scattering of the electromagnetic (EM) waves on the individual surface features. In [11] the transmission spectra of submicron-scaled (period is 1.17 μm) silicon/silica 1D photonic crystals with surface roughness were investigated theoretically and experimentally. The simulations, made by TMM applying the homogenization approximation, showed disorder-induced narrowing of the lowest band gap and smearing of the band edges. The experiment confirmed the effects well with the exception of the shift of the upper band edge which is larger than predicted by the calculations.

Thus, in view of these partly controversial results even for the simplest periodic structure—the 1D PhC—the influence of disorder on the photonic band structure is still a topical problem. The main points of interest in our opinion are the mechanism of the band gap smearing, estimation of the amount of disorder under which a PhC still exhibits band gaps and determination of the relation between transmission, reflection, and scattering.

In this publication we present both theoretical and experimental investigations on 1D dielectric photonic crystals with *surface roughness*. Transmission experiments were performed in the microwave region on a mm-sized structure with roughness of the order of 10%. Because of the large dimensions it is possible to design the roughness instead of having to consider it as a fabrication-related feature. Due to the scalability of Maxwell's equations the main conclusions are valid for down-sized structures like submicron-sized photonic crystals for the near infrared and visible part of the spectrum.

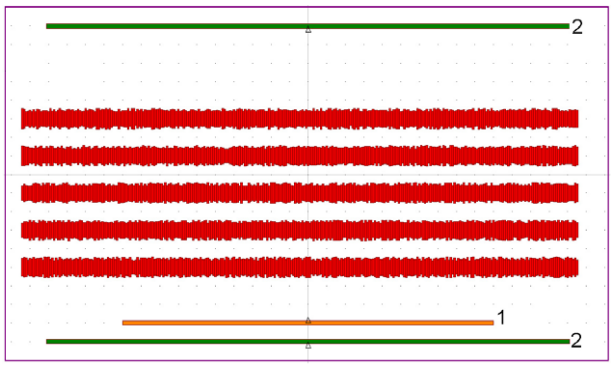

Figure 1. General view of the problem. The horizontal bar 1 is the source. The bars 2 are the monitors.

2. Description of the model

An important point is to define the surface roughness in a clear and reproducible way consistent with the sample used in the experiment. In our model we consider each high-index layer of a PhC as being composed of thin bars with the same width. In the case of a structurally perfect photonic crystal with zero roughness all these bars have the same length. The surface roughness is created by a random change of the length of each bar (figure 1). In figure 1 the horizontal bar 1 represents the 'source' which emits a plane wave only in the direction of the PhC. The horizontal bars 2 are transparent 'monitors' which record the EM energy flux as a function of time. The frame shows the edge of the computational domain with perfectly matched layers, i.e. totally absorbing boundaries.

Mathematically the roughness is introduced in the following way: the lengths of the bars (l_{bar}) are varied randomly around the length in the perfect structure (l_{h}) according to

$$l_{\mathrm{bar}} = l_{\mathrm{h}}(1 + \delta \cdot P_{-1;1}). \tag{1}$$

$P_{-1;1}$ is a uniformly distributed random value in the range $[-\mathbf{1}; \mathbf{1}]$, and δ is the roughness amplitude. As an example, for $\delta = 0.1$ the value of l_{bar} varies between $0.9l_{\mathrm{h}}$ and $1.1l_{\mathrm{h}}$. The position of the center of each bar is the same as in the perfect PhC. The top and the bottom sides of each layer have the same roughness profile. The roughness profiles are different for the different layers. This corresponds to five different realizations of roughness within one PhC. Therefore, we suppose that the roughness being the same on both sides of a layer is not significant for the effects of surface roughness. The scheme of a part of a layer with roughness is depicted in figure 2.

The simulations (in accordance with the PhC in the experiments) were carried out for a five-layer dielectric–air structure with the following parameters: thickness of the dielectric layers is 1.11 mm, the air spacings between the plates are 1.21 mm which corresponds to a period of the structure of $a = 2.32$ mm. The total number of bars in each layer (N_{R}) defines the 'roughness resolution'. Table 1 shows the correspondence between the resolution and width of a single bar in our model. The total width of the layers in the model is 15a or approximately 35 mm; in the experiment the lateral dimensions of the plates are 24 mm × 39 mm. The dielectric

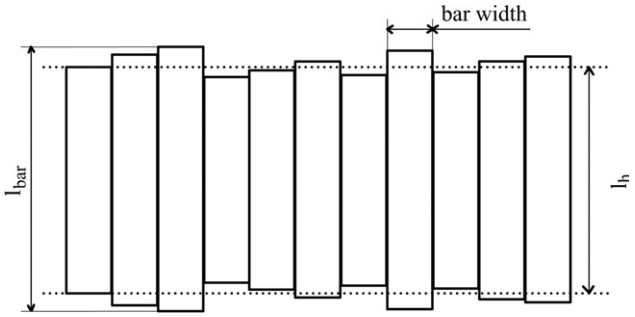

Figure 2. The scheme of a part of a layer with roughness used in our model.

Table 1. Roughness resolution.

Resolution (number of the bars in each layer)	The width of a single bar (mm)
$N_R = 150$	0.232
$N_R = 300$	0.116
$N_R = 600$	0.058

constant was assumed to be 9.86 since ultrapure alumina was used as the dielectric material in the experiment and this value gave the best fit to the experimental spectrum of the structurally perfect PhC.

The transmission spectra were calculated by means of Rsoft FullWAVE™ [12] commercial package involving two techniques: direct finite-difference-time-domain (FDTD) calculations (section 5) and FDTD calculations followed by a fast Fourier transform (section 3). In the latter case a Gaussian pulse excitation is used. A monitor records the energy flux as a function of time and then the fast Fourier transform (FFT) is applied to this function. As a result we obtain a transmission spectrum normalized to the power emitted by the source. The dimension of the FDTD computational cell is $1/128$ with respect to the period of the PhC. We have tested the problem also on a $1/256$ grid but no difference in the results was observed. Using the FFT to calculate transmission spectra can result in some numerical artifacts for low frequencies, since a time limit is set for the calculations time. In order to check the range of validity, the transmission of the structurally perfect structure was also simulated by the MULTEM2 [13] program utilizing the multiple scattering method. The very good coincidence observed for the perfect structure between FullWAVE™ and MULTEM2 spectra for frequencies above 5 GHz confirms that we have chosen a sufficiently fine grid and a sufficiently long calculation time in our FDTD calculations. This is also valid for the simulations of PhCs with roughness where MULTEM2 is not applicable.

The model described above is a two-dimensional model. However, we expect that deviations from results of a three-dimensional model are small. Reasons are: (a) the transmission is averaged over 10 different realizations of the roughness (see figures 3 and 4 below). This can be considered as being equivalent to 10 layers on top of each other in the third direction. That way the roughness varying in the third dimension is taken into account to some extent. (b) However, from the edges of a PhC extended in the third direction some light would be scattered which is not detected by the monitors of the two-dimensional calculation. This will not affect the general spectral features, it can only cause a lower transmission or reflection than calculated in the two-dimensional model. See figure 7 and the remark at the end of section 4.

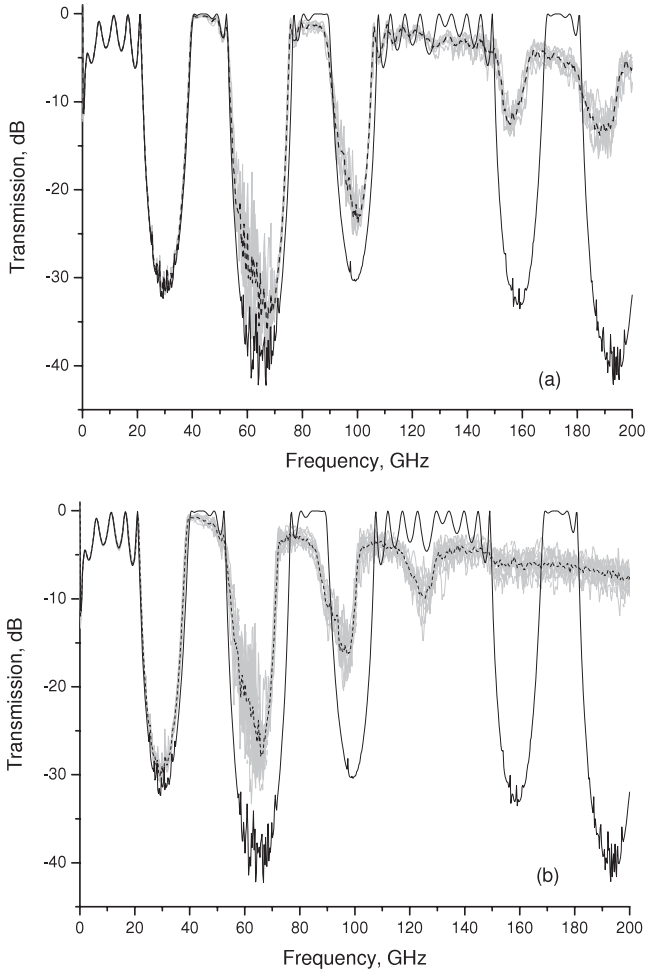

Figure 3. Normal-incidence transmission spectra of the 1D PhC with surface roughness: $\delta = 0.2$, $N_R = 300$ (a); $\delta = 0.4$, $N_R = 300$ (b). Solid black curve: zero-roughness structure; gray curves: 10 different realizations of surface roughness with the same δ; dashed black curve: the transmission averaged over the ensemble of the 10 realizations. 100 GHz corresponds to a reduced frequency $\omega a/2\pi c = 0.77$.

3. Calculated transmission spectra

In figure 3 the calculated transmission spectra for the geometry of figure 1 are shown. We present here the following cases: $\delta = 0.2$, $N_R = 300$ (figure 3(a)); $\delta_1 = 0.4$, $N_R = 300$ (figure 3(b)). The solid black curve shows the transmission of the zero-roughness structure with the thickness of the high-index layers $l_h = 1.11$ mm. The dashed black curve shows the transmission averaged over an ensemble of 10 structures with the same δ (thin gray curves). The frequency 100 GHz corresponds to a reduced frequency $\omega a/2\pi c = 0.77$.

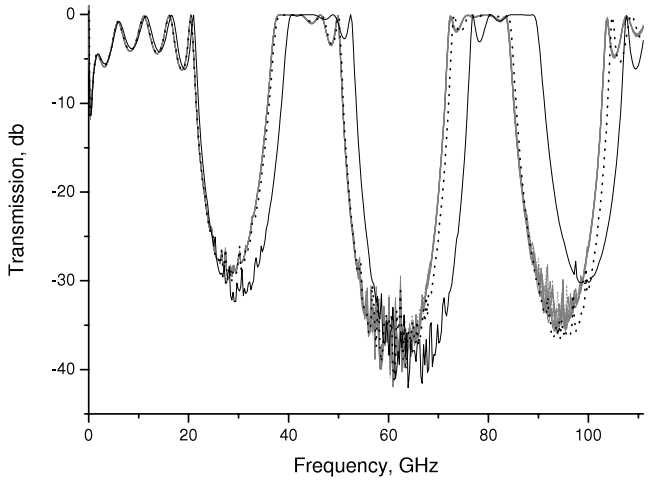

Figure 4. The 'experiment-oriented' simulation, $l_h = 1.19$ mm, $\delta = 0.06$, $N_R = 600$. Solid black curve: perfect structure ($l_h = 1.11$ mm); dotted black curve: perfect structure with increased thickness ($l_h = 1.19$ mm); gray curves: 10 different realizations of surface roughness with the same δ.

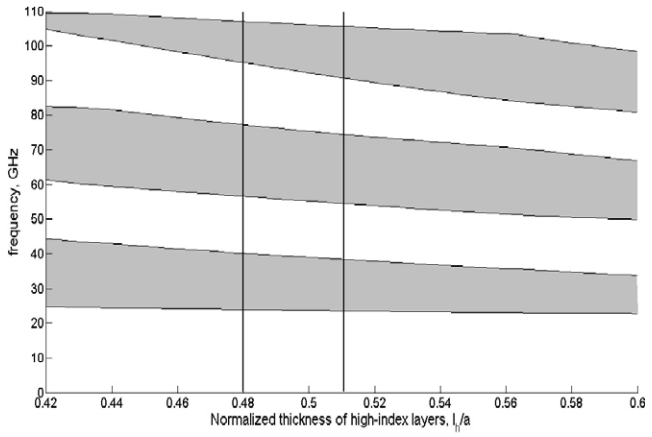

Figure 5. The gap map of a perfect 1D PhC. The x-axis is the thickness of high-index layers in units of the lattice constant. The band gaps are the shaded regions. The left and the right vertical lines correspond to the values of l_h used for calculations of the black solid and black dotted lines in figure 4, respectively. The lattice constant is $a = 2.32$ mm.

It is clearly seen from figure 3 that the surface roughness practically does not affect the lowest band gap even for $\delta = 0.4$ (figure 3(b)). However, the higher the frequency the higher is the effect of the surface roughness. The gaps shrink, the interference structure within the transmission bands is smeared out, and the fine structure of the spectra depends on the details of the realization of the roughness. This is easily understandable since the frequency of the center of the first band gap (34 GHz) corresponds to a wavelength $\lambda/n = 2.8$ mm that is more than 10 times larger than the size of the roughness features. The center of the third band gap (100 GHz) corresponds to a wavelength of $\lambda/n = 0.96$ mm that closely approaches the order of the dimensions of the roughness features.

We therefore conclude that the main effect of surface roughness—scattering of the plane wave on surface features—becomes significant if $\lambda/n \sim l_h \cdot \delta$, where n is the refractive index of the high-index layers ($n = 3.14$ for ultrapure alumina). We shall consider the scattering processes in more detail in section 5.

In the experiment (section 4) the surface roughness is realized by gluing alumina powder to both sides of each plate. Obviously, in order to simulate such a structure we have to take into account the fact that the average thickness of each plate is now higher compared to the case without the powder. In other words, since we always keep the lattice constant unchanged, the air filling fraction in the experimental structure with roughness will be lower compare to the zero-roughness case. According to the experimental roughness parameters, which are described in the next section, we have used the following parameters for 'experiment-oriented' simulation (figure 4, gray curves): $l_h = 1.19$ mm, $\delta = 0.06$, $N_R = 600$. From the microscopic inspection we conclude that a thin layer of glue on the surface of the plates has also to be taken into account. In the simulation its thickness is 35 μm and its dielectric constant 2.25. With these values the overall agreement is very good, particularly for the band width and the positions of the band edges.

The increased average thickness of the high-index layers results in a significant shift of the entire spectrum to lower frequencies compare to initial structure with $l_h = 1.11$ mm. At the same time δ is small and the effect of the details of the disorder is nearly negligible since the 10 different realizations represented by gray curves give practically the same spectra.

In order to elucidate the shifts of the characteristic features in the transmission curves of figure 4 we plot the dependence of the three lowest gaps on layer thickness for a perfect 1D PhC (figure 5). This gap map was calculated by the plane-wave-expansion method using BandSOLVE™ [12] commercial package. A cross-section made at the left vertical line shows the positions and widths of the gaps that correspond to the solid black transmission curve in figure 4. The right vertical line indicates the situation for the black dotted curve in figure 4 calculated for a zero-roughness structure with increased layers thickness of $l_h = 1.19$ mm.

Thus, for the experiment-oriented simulation two separate effects contribute: (i) a 'red-shift' of the photonic band structure due to the increase of the average thickness of the high-index plates and (ii) the scattering of EM waves at the surface features which are introduced by formula (1).

We explore here mainly the $N_R = 300$ case. The differences seen for resolutions $N_R = 150$ and 600 are only quantitative but not qualitative, namely the effect of surface roughness is more pronounced in the former case and less pronounced in the latter one with respect to $N_R = 300$.

We have also simulated a 10-layer structure with the same parameters as well as 1D PhCs with higher refractive index contrasts. These additional results show that the conclusions are generally valid for a variety of 1D PhC.

4. Transmission experiments

In order to test the results of the model calculation we performed an 'experimental simulation' in the frequency range

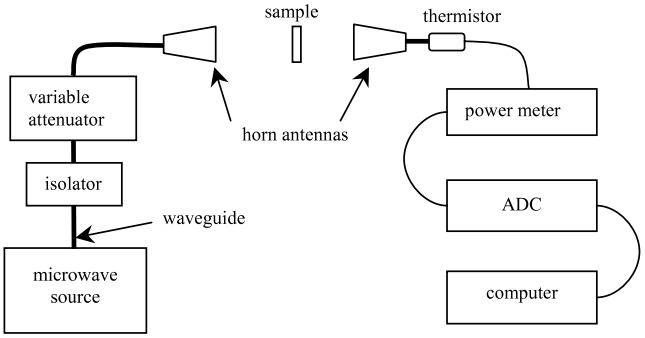

Figure 6. Schematic description of the experimental setup.

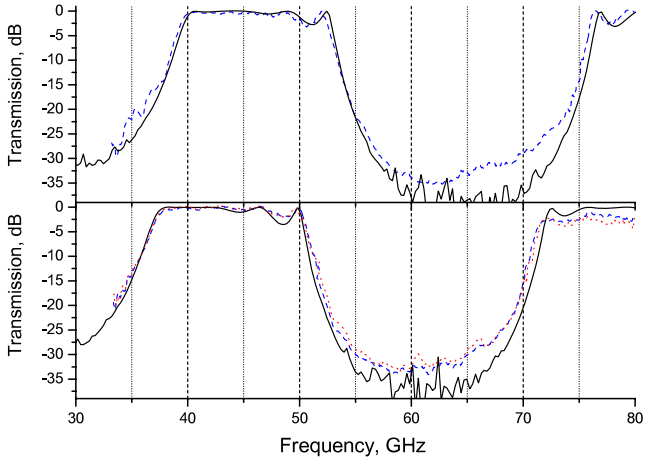

Figure 7. The transmission spectra in the range 33–80 GHz. Upper plot: transmission of a PhC with zero roughness, blue dashed curve is experimental, black solid curve is calculated. Lower plot: transmission of a structure with roughness, blue dashed and red dotted curves represent two experimental transmission curves for two different samples with the same kind of powder; the black solid curve is the simulated transmission of a PhC with roughness taken from figure 4.

around the second transmission band. For this purpose test samples of a 1D PhC with surface roughness were fabricated. They consist of five alumina plates separated by air with thicknesses given in section 2. With these dimensions the lowest transmission bands are in the microwave range of the electromagnetic spectrum. The surface roughness was created by gluing alumina powder to both surfaces of each plate.

For the determination of the roughness we used optical microscopy and profilometry. Additionally, atomic force microscopy was used for the surface of the uncovered alumina plates whose rms roughness was found to be 0.7 μm. This is considered to be negligible in the present context. In the optical microscopy the grain size of the alumina powder was found to vary from 30 to 150 μm; about 75% of the grains are distributed in the range 60–90 μm, however. According to the profilometry measurements, the peak-to-peak variation of the profile was 70 μm. The parameters for the best fit to the experimental results are given below.

Transmission of the test sample was measured in the microwave Q-band (33–50 GHz) and V-band (50–75 GHz) using backward wave oscillator sources, Siemens RWO-50S and RWO-75S, respectively. The scheme of the experimental setup is presented in figure 6. Due to the use of the horn antennas the direction of EM wave propagation is essentially normal to the surface of the PhC. Within the band gap regions the transmission was measured with increased sensitivity of the power meter in order to obtain a better signal-to-noise ratio.

The experimental and simulated transmission spectra in the range 33–80 GHz are joined in figure 7. In the upper plot the experimental (blue curve) and theoretical (black curve) transmission for zero-roughness PhC are presented. The lower plot shows two experimental transmission curves (blue and red) for two different samples with the same kind of powder and theoretical transmission of PhC with roughness (black) taken from figure 4, namely for the following simulation parameters: $l_h = 1.19$ mm, $\delta = 0.06$, $N_R = 600$. Additionally, we take into account the existence of a layer of glue on the surface with thickness 35 μm and dielectric constant of 2.25. The overall agreement is considered as very good, particularly for the band width and the positions of the band edges. However, in the upper band for frequencies above 72 GHz the experimental transmission is slightly lower than simulated. This discrepancy might be due to the fact that we considered the 2D model, so scattering in the third dimension was not taken into account.

5. Simulation of wave propagation

In order to get a deeper insight into the processes of the scattering of the electromagnetic waves in roughened 1D photonic crystals field distribution patterns obtained by FDTD calculations are investigated. Since in this case the PhC is irradiated by a monochromatic wave there are two important cases: the frequency lies (i) in a band gap or (ii) in a transmission band.

It is also very interesting to investigate the dependence of transmission spectra on the geometry of the problem. Due to the scattering the detected transmission may depend on the positions of the monitors and their dimensions with respect to the period of the structure and the wavelength.

In figure 8 the EM field distribution patterns are shown for a frequency of the source situated in the center of the second gap (64 GHz) for a perfect structure (a) and for a PhC with roughness amplitude $\delta = 0.4$ (b). It should be outlined that surface roughness with $\delta = 0.4$ is too high to simulate any actually observed fabrication imperfections. We explore the case here in order to obtain more pronounced scattering effects and to observe their influence on the band gaps. There are two pairs of monitors used now, one pair is located near the sample and records 'near-field' transmission and reflection. The other pair records the 'far-field' transmission and reflection. In the case of the perfect PhC the near-field transmission and reflection are 0.03% and 99.7%, respectively, whereas in far-field the transmission is 0.01% and the reflection is 98.7%. Ideally, in the absence of absorption and scattering the sum of transmission and reflection must be 100%. However, in our calculations we have small deviations due to the diffraction effects at the edges of the generated beam and due to the finite lateral size of the PhC. The roughened photonic crystal (figure 8(b)) still exhibits high reflection. Quantitatively, the

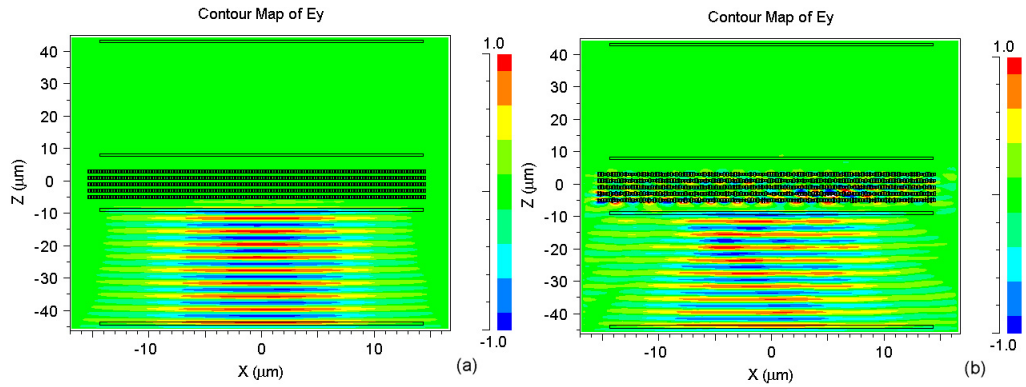

Figure 8. The field distribution patterns for a perfect PhC (a) and for a PhC with roughness amplitude $\delta = 0.4$ (b). There are two pairs of monitors on each plot, one pair is located near the sample and records 'near-field' transmission and reflection, the other pair records 'far-field' transmission and refection. In all the cases a plane wave is generated by the source located at $z = -8$ μm and propagates only toward the PhC. The frequency of the wave is 64 GHz (vacuum wavelength $\lambda = 4.66$ mm). It corresponds to the center of the second gap.

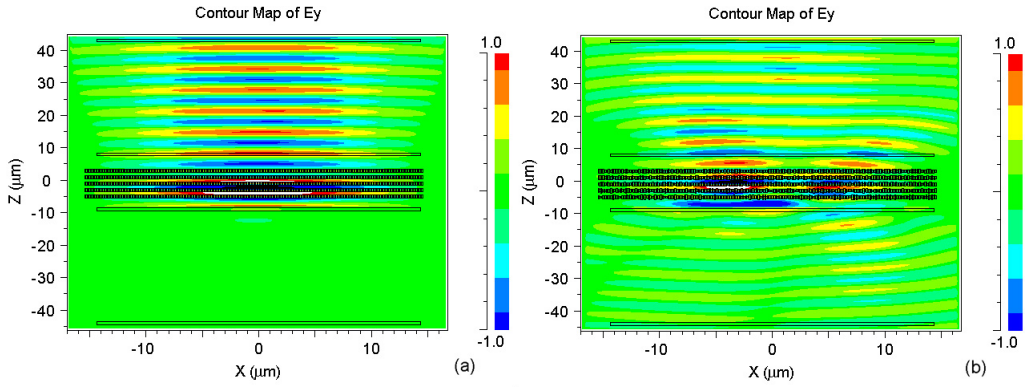

Figure 9. The same as in figure 8 but for a frequency of 40 GHz ($\lambda = 7.5$ mm) in the second transmission band.

near-field transmission and reflection now are 0.6% and 90%, respectively. The far-field transmission is 0.35% and the reflection is 89%.

The field pattern for the same structure but for the frequency within the second transmission band (40 GHz) is shown in figure 9. In the case of zero roughness the transmission and reflection are 98% and 1.5% for near-field and 94% and 1.3% for far-field, respectively, whereas in the roughened PhC they are 70% and 29% for near-field and 53.9% and 15.4% for far-field. Although the wavelength is larger than in the previous case (frequency in a band gap) the effect of the surface roughness is much more pronounced. We believe that the reason is that in the center of a band gap the wave penetrates only for the first few layers and thus encounters less scattering than the transmitted wave. Note, that the reflected wave is not a pure plane wave since the mechanism of reflection now is backscattering from surface features but not interferential suppression as in the case of a gap. Thus, in the presence of scattering, for an appropriate comparison of the experimental and theoretical data, the distance from the sample to the monitor has to be taken into account since the farther the detector is away from the sample the less scattered waves will be detected. These 'lost' scattered waves are the reason for transmission and reflection not adding up to 100%.

6. Conclusions

The results of the simulations and the comparison with the experimental data give rise to the following conclusions:

- The effect of surface roughness on the position and width of *the lowest band gap* is negligible if an average thickness equal to the thickness of a structurally perfect PhC is used.
- For the second and third gap the depth of the transmission minimum and the width are reduced with increasing roughness but the gaps are still clearly seen even for a roughness parameter as large as $\delta = 0.4$.
- For equal δ the surface roughness has stronger influence on the transmission and reflection for lower resolution (larger feature sizes of the roughness).
- The effect of disorder gets stronger at shorter wavelengths and becomes significant when $\lambda/n \sim l_h\delta$, where n and l_h are the refractive index and thickness of the high-index layers, respectively.
- Our simulations show that in the presence of the roughness-induced scattering the distances between the sample and the monitors can also influence the values of the transmission and reflection detected. When a monitor is located close to the sample the major part of the scattered power will be recorded. In far-field

measurements more of the scattered power will be missed and transmission and reflection will not add up to 100%.
- An inexact determination of the thickness of the layers causes a higher inaccuracy in the calculated positions of spectral features than details of the surface roughness.
- Due to the scalability of Maxwell's equations one can extend our results to submicron-sized 1D photonic crystals and state that the lowest bands and gap remain unchanged for any reasonable amount of fabrication imperfections during growth or structurization.

Acknowledgments

This work was supported by the Austrian Nanoinitiative, project PLATON N1104. The authors would like to acknowledge F J Schmied for AFM measurements.

References

[1] Yablonovich E 1987 *Phys. Rev. Lett.* **58** 2059
John S 1987 *Phys. Rev.* B **58** 2486
[2] Ho K M, Chan C T and Soukoulis C M 1990 *Phys. Rev. Lett.* **65** 3152
Shang Z and Satpathy S 1990 *Phys. Rev. Lett.* **65** 2650
Leung K M and Liu Y F 1990 *Phys. Rev. Lett.* **65** 2646
[3] McCall S L and Platzman P M 1991 *Phys. Rev. Lett.* **67** 2017
Yablonovich E, Gmitter T J and Leung K M 1991 *Phys. Rev. Lett.* **67** 2295
[4] Tolmachev V A, Perova T S, Pilyugina J A and Moore R A 2006 *Opt. Commun.* **259** 104
[5] Li H, Chen H and Qiu X 2000 *Physica* B **279** 164
[6] Kaliteevski M A, Beggs D M, Brand S, Abram R A and Nikolaev V V 2006 *Phys. Rev.* E **73** 056616
[7] Kaliteevski M A, Beggs D M, Brand S, Abram R A and Nikolaev V V 2006 *Phys. Rev.* B **73** 033106
[8] Sozuer H S and Sevim K 2005 *Phys. Rev.* B **72** 195101
[9] Maskaly K R, Maskaly G R, Carter W C and Maxwell J L 2004 *Opt. Lett.* **29** 2791
[10] Maskaly K R, Carter W C, Averitt R D and Maxwell J L 2005 *Opt. Lett.* **30** 2930
[11] Jaksic Z *et al* 2006 *Microelectron. Eng.* **83** 1792
[12] http://www.rsoftdesign.com/
[13] Stefanou N, Yannopapas V and Modinos A 2000 *Comput. Phys. Commun.* **132** 189